Journal of Power Sources 237 (2013) 325–331

Contents lists available at SciVerse ScienceDirect

Journal of Power Sources

journal homepage: www.elsevier.com/locate/jpowsour

Active carbon wrapped carbon nanotube buckypaper for the electrode of electrochemical supercapacitors

Hongyuan Chen [a,b], Jiangtao Di [a,b], Yu Jin [a,c], Minghai Chen [a,*], Jing Tian [a,b], Qingwen Li [a,**]

[a] Suzhou Institute of Nano-tech and Nano-bionics, Chinese Academy of Sciences, Suzhou 215123, PR China
[b] Graduate University of Chinese Academy of Sciences, Beijing 100049, PR China
[c] School of Materials Science and Engineering, Hefei University of Technology, Hefei 230009, China

HIGHLIGHTS

- We fabricated novel CNT@active carbon core-shell structural nanowire buckypaper.
- The synthetical method was facile.
- Active carbon and CNT had good contact.
- The composite buckypaper showed good electrochemical performance as the electrodes of supercapacitors.
- The electrochemical performance of active carbon was furthest exerted in this structure.

ARTICLE INFO

Article history:
Received 7 November 2012
Received in revised form
25 February 2013
Accepted 28 February 2013
Available online 14 March 2013

Keywords:
Electrochemical capacitor
Carbon nanotube buckypaper
Active carbon
Core-shell structure
Electrode

ABSTRACT

Active carbon (AC) is a widely used electrode material for electrochemical double layer capacitors (EDLCs). However, it often shows poor rate capability due to its low conductivity. Herein, we report a binder-free carbon nanomaterials hybrid structure formed by core-shell structural nanowire network, in which carbon nanotube (CNT) buckypaper serves as conductive scaffold and porous AC layer is coated on individual CNTs in the buckypapers as active component for capacitance contribution. Such hybrid structure shows a greatly enhanced rate performance compared to pure CNT and AC electrode with its electrochemical capacitance better than its two components at large charge/discharge current densities. The AC layer in this hybrid buckypaper, which is as the main component contributed to the electrochemical capacitance, shows good rate performance and enhanced electrochemical capacitance at large current density. The performance improvement arises from the integration of resultant highly porous AC layer, conducting network and good interfacial contact between AC coating and CNTs, favoring the efficient transport of ions and electrons over the electrode surface. Moreover, the assembled EDLC with such hybrid buckypaper electrode also present higher and more stable energy densities with the increase of power densities compared to AC based EDLC.

1. Introduction

Recently, electrochemical capacitors have attracted increasing attention due to the rapidly growing need for clean energy sources, as it can provide high power density, fast charge/discharge rate and long cycle lifetime [1]. Electrochemical double layer capacitors (EDLCs) using carbonaceous materials as electrodes are extensively developed due to their low cost and high operation stability [2,3]. Among them, active carbon (AC) with large specific surface area is widely employed [4–6]. However, its poor conductivity arising from non-graphitized structure has limited its charge/discharge performance at high charge/discharge current densities. Therefore a variety of approaches has been developed to make AC electrodes more conductive by mixing with highly conductive materials such as graphene [7–9] and carbon nanotube (CNT) [10–14]. Yet it still faces up with the problem on the diffusion of electrolyte [15–17]. Moreover, the non-uniform dispersion of the conducting additives and therefore poor contact with AC particle interfaces also limit the diffusion and transport of electrons over the electrode to some extent [11]. Although an AC coated CNT paper which had been developed could solve the problem, the use of low conductive organic binder such as polyvinylidene fluoride for electrode

* Corresponding author. Tel./fax: +86 512 62872552.
** Corresponding author. Tel.: +86 512 62872577; fax: +86 512 62872552.
E-mail addresses: mhchen2008@sinano.ac.cn (M. Chen), qwli2007@sinano.ac.cn (Q. Li).

0378-7753/$ – see front matter © 2013 Elsevier B.V. All rights reserved.
http://dx.doi.org/10.1016/j.jpowsour.2013.02.082

assembly was found to limit the electrochemical performance improvement of the electrode [13].

Herein, we proposed an architecture as a high-performance electrode, in which a CNT buckypaper served as a conducting scaffold and pyrolyzed thin-layer AC coated on individual nanotubes acted as active layers (AC coated CNT paper). This structure was proved to help utilize the mechanical robustness and high conductivity of the buckypaper and meanwhile the excellent electrochemical capacitive performance of AC. Importantly, the hybrid electrode could be prepared free of binders. Thus it showed an enhanced electrochemical capacitance, especially at high current densities. Moreover, the network structure maintained a large number of interconnected porous channels in the electrode, which favor sufficient ion transportation paths for the diffusion of electrolyte. These unique features are therefore of significant importance for the hybrid buckypaper achieving high energy density and high power density simultaneously.

2. Experimental

Large-diameter multi-walled CNTs (MWCNTs) were synthesized by floating catalyst chemical vapor deposition (FCCVD) method with ferrocene as the catalyst and toluene as the carbon source [18]. Polyacrylonitrile (PAN, $M_w = 230{,}000$) was purchased from Goodfollow Company Inc. Zinc acetate ($Zn(CH_2COO)_2 \cdot 2H_2O$), *N*,*N*-dimethylformamide (DMF) and nitric acid (HNO_3) were purchased from Sinopharm Chemical Reagent Co., Ltd. All materials were directly used as received without further purification. The pristine buckypaper with a uniform network structure was prepared by vacuum filtration of the MWCNT aqueous dispersion [19].

To prepare AC coated CNT buckypaper, the CNT buckypaper was firstly immersed into the PAN/$Zn(Ac)_2$–DMF precursor solution with different concentration. The mass ratio of PAN and $Zn(Ac)_2$ was kept as 2:5, while the concentration of the solution was controlled by changing the total mass of PAN and $Zn(Ac)_2$. Pristine PAN/$Zn(Ac)_2$–DMF solution was also cast on a glass substrate to prepare pristine AC as a comparison. All of the buckypapers immersed by the precursor were carbonized by the same process as below: pre-oxidation by air at 300 °C for 120 min and then carbonization at 850 °C for 100 min in argon [20]. Then the nanotubes in the buckypaper were uniformly coated with a layer of AC, forming a core-shell structure. $Zn(Ac)_2$ was added here as a pore-creator and activating reagent, which can be decomposed into zinc oxide by the process of carbonization [21]. The carbonized samples were immersed into 1 M HNO_3 for 48 h to remove zinc oxide in the AC layer, and then they were washed by deionized water for several times to remove the remnant HNO_3. After being dried, freestanding buckypapers coated by AC were obtained. The fabrication process and the structure of the electrode are shown in Fig. 1.

The morphologies and structures of the samples were characterized by transmission electron microscopy (TEM) (Tecnai G2 F20 S-Twin, FEI) and scanning electron microscopy (SEM) (Quanta 400 FEG, FEI). Raman spectrum was recorded on a LabRAM HR Raman spectrometer (HORIBA Jobin Yvon). Sheet resistance (R_s) of the samples was measured by using an ST-2258A multifunction digital four-probe tester (Suzhou Jingge Electronic co., Ltd.) and the electric conductivity (σ) of the samples was calculated according to the relationship: $\sigma = 1/(R_s \cdot t)$, where t is the thickness of the samples. Nitrogen sorption isotherms were measured at 77 K with a Micromertics ASAP 2020 Automatic Physisorption Analyzer (Micromertics, USA), before measurements, the samples were degassed in a vacuum at 160 °C for at least 5 h. The Brunauer–Emmett–Teller (BET) method and the Barrett–Joyner–Halenda (BJH) model were utilized to calculate the BET specific surface areas and the pore size distributions, respectively.

The electrochemical measurements were performed in three-electrode system by using a CHI 660C electrochemical workstation interfaced to a computer system with corresponding electrochemical software. The samples were tested in a potential range

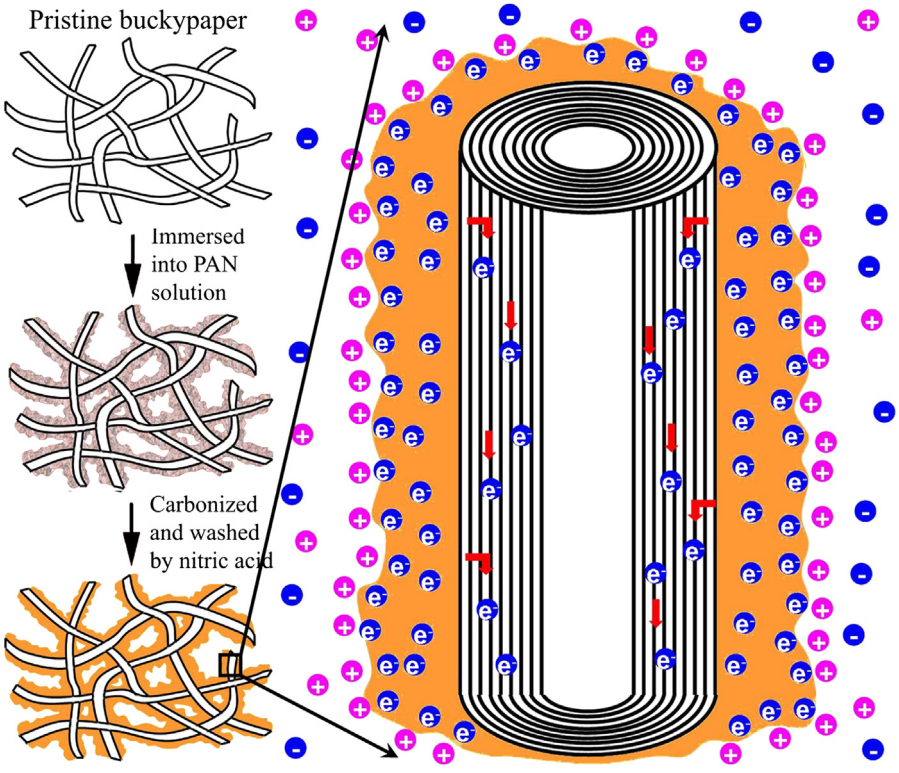

Fig. 1. Schematic of the preparation procedure for AC coated CNT buckypaper and its electrochemical performance benefits.

of −1 to 0 V in 6 M KOH aqueous solution as electrolyte. A platinum wire and a saturated calomel electrode (SCE) were used as the counter electrode and the reference electrode, respectively. The galvanostatic charge/discharge curves were performed at current densities of 0.5, 1, 2, 5 and 10 A g^{-1}. The specific capacitance in this study was calculated based on the whole mass of the composite buckypaper but not only active carbon on it.

A symmetrical supercapacitor was assembled by using the 25 wt.% AC coated buckypapers as the opposite electrodes and 6 M KOH aqueous solution as the electrolyte. A piece of porous PE membrane for Li-ion battery was soaked by 6 M KOH aqueous solution to be the separator of the supercapacitor. The electrochemical performances of the supercapacitor were tested with an operating voltage of 1.5 V. Energy density (E) and power density (P) were calculated from CV curves according to Equations (1) and (2). They are as followed:

$$E = \frac{1}{2}CV^2 \quad (1)$$

$$P = \frac{E}{t} \quad (2)$$

where C is the specific capacitance, F g^{-1}; V is the potential drop, V; t is the discharge time, s.

3. Results and discussion

Fig. 2 shows the structural details of a pristine buckypaper before and after AC coating. Fig. 2(a) and (d) displays that the surface of the buckypaper became coarse and grey after the coating of AC. The CNTs in a pristine buckypaper are thick and well-crystallized with detailed structural characterization provided in Fig. 2(b) and (c). After coating procedure, the CNT network remained well but the diameter of individual tubes became obviously larger (Fig. 2(e) and (f)). A further characterization by TEM shows that the pristine CNTs prepared by FCCVD have large diameter between 30 and 150 nm with tens of walls (see Fig. 3(a)). Furthermore, they show clear walls and clean surface in Fig. 3(b). However, the blurry crystal lattice and the rough surface of the CNTs could be seen after being coated with AC shown in Fig. 3(c) and (d). It reveals the formation of a typical core-shell structure. The shell is a layer of AC and the core is the nanotubes. The thickness of the outer layer depends on the concentration of the carbon precursor solution used for impregnation and is in the range of

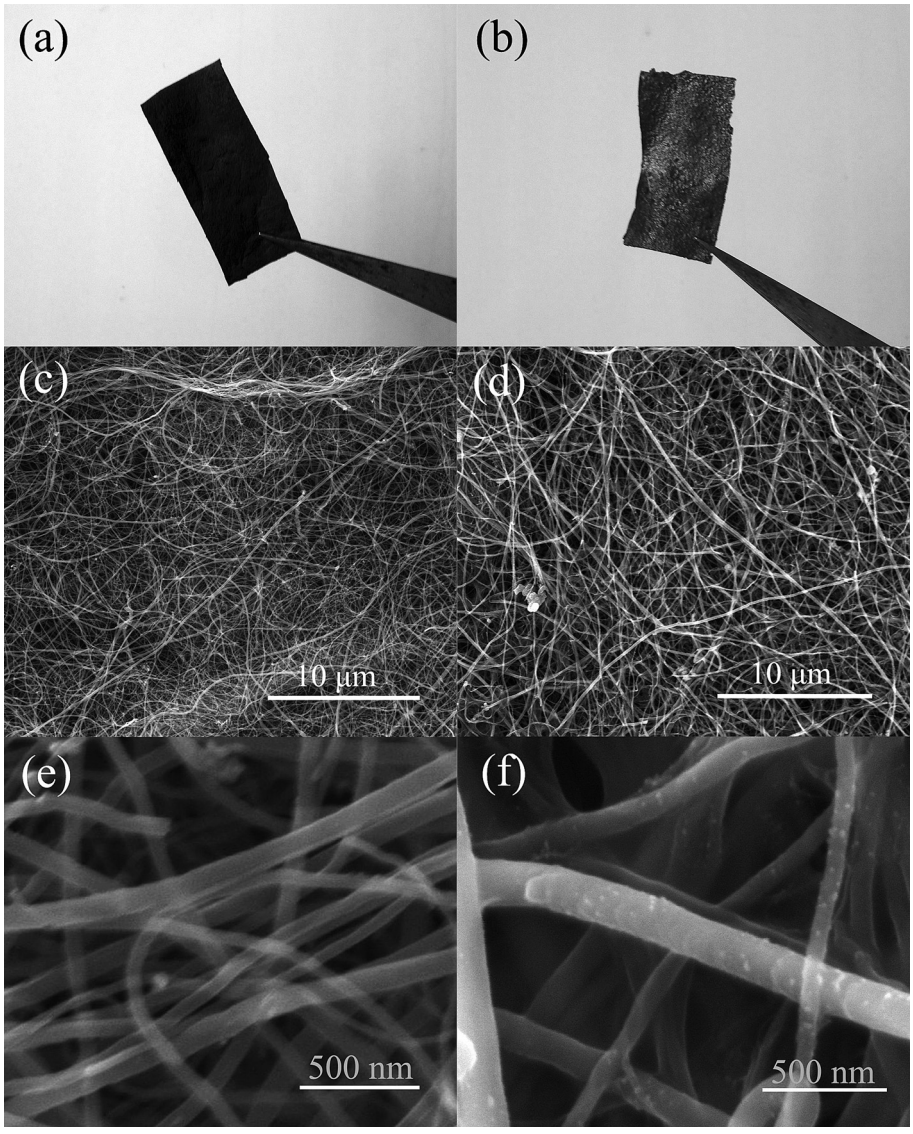

Fig. 2. Optical photographs (a and d) and SEM images (b, c, e, f) of pristine CNT buckypaper (a–c) and 25 wt.% AC coated buckypaper (d–f).

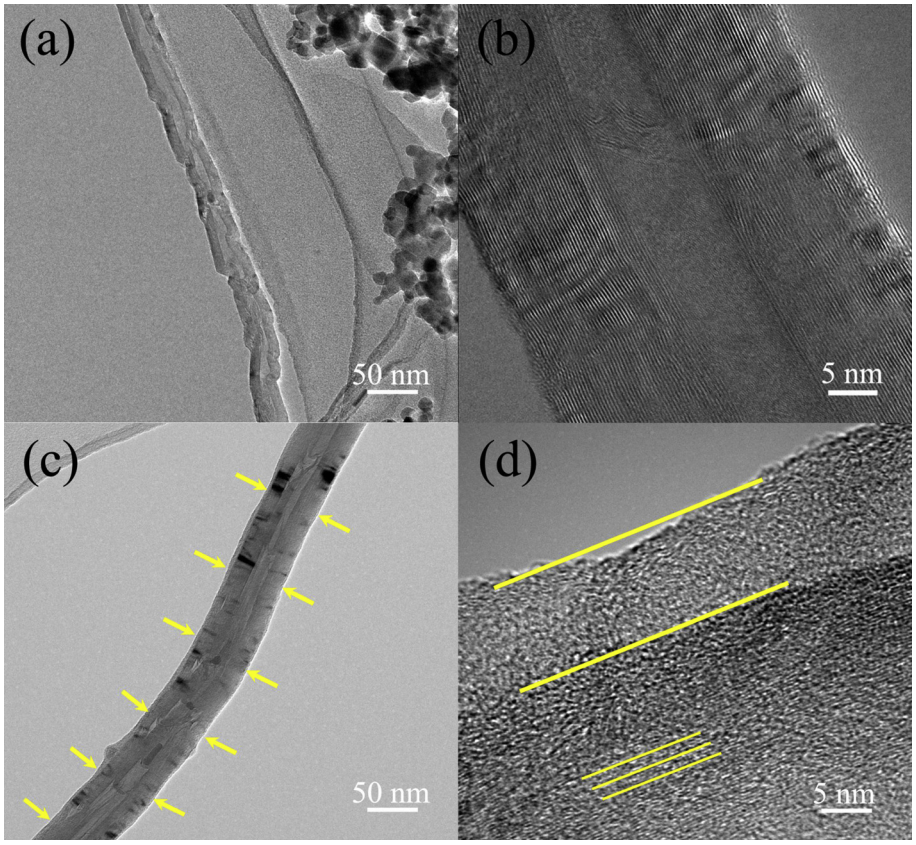

Fig. 3. TEM images of CNT structures before (a, b) and after AC coating (c, d).

several nanometers. The weight percentage of AC coated on CNT buckypaper can be estimated according to the correlation curve provided in Fig. S1.

Fig. 4 shows the electrical conductivities and structural properties of the hybrid buckypapers. The coating of AC led to the decrease of electrical conductivity of the buckypaper for its intrinsic poorer conductivity than CNTs. Fig. 4(a) shows the effect of AC weight percentage on the conductivity of the hybrid buckypapers. The conductivity of the AC coated CNT buckypaper decreased with increasing the wrapping percentage (wt.%) of AC

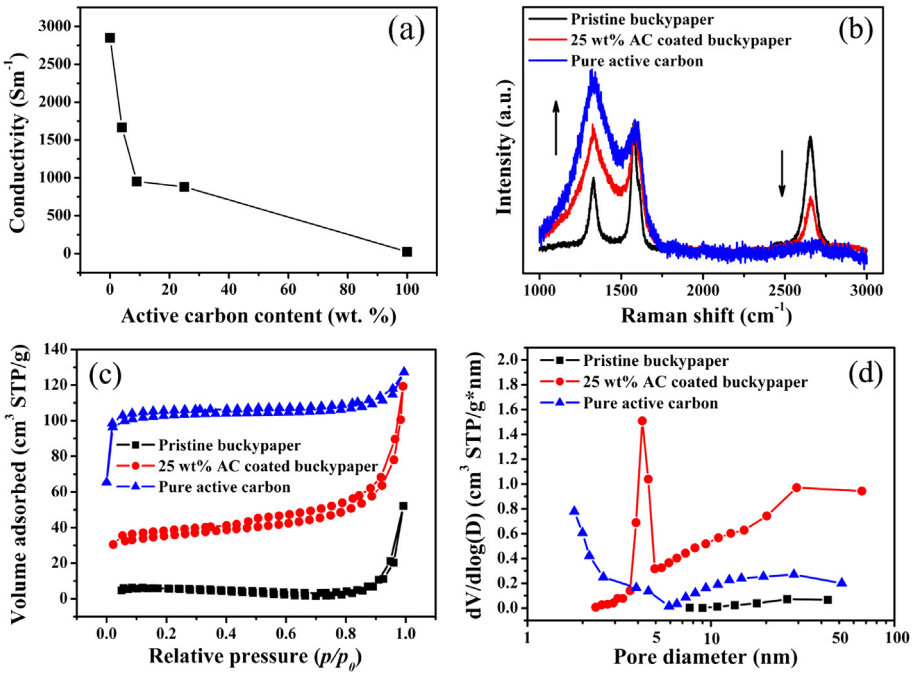

Fig. 4. The electrical conductivity (a) and Raman spectra (b) of the buckypapers loading with different percent of active carbon; N2 sorption isotherms (c) and pore size distribution curves (d) for pristine buckypaper, active carbon coated buckypaper and pure active carbon.

showing a nonlinear feature. The more AC was loaded on the buckypaper, the lower conductivity the buckypaper would have. When the AC wrapping weight percentage was in a range from 15 to 30 wt.%, the conductivity of the hybrid buckypaper dropped slowly. The conductivity for the hybrid buckypaper with 25 wt.% AC is at 880 Sm^{-1}, much higher than that of pure AC (24 Sm^{-1}) prepared by the same procedure in the absence of CNT buckypaper. As a result, AC coated buckypaper showed much improved capability on electronic transport compared with the pure AC, which may ensure better performance for EDLC [22].

Fig. 4(b) compares the Raman spectra of the CNT buckypaper before and after AC coating. A high *G*/*D* ratio with a strong 2D-band for the CNT buckypaper indicates that the nanotubes are well-crystallized [23,24]. In contrast, pure AC presents a low *G*/*D* ratio and nearly no 2D-band, revealing the formation of amorphous carbon [25]. When the buckypaper was coated with 25 wt.% AC (noted as 25 wt.% AC coated buckypaper), its Raman spectrum shows an interim feature between the pristine buckypaper and pure AC, further confirming the introduction of AC wrapping. Fig. 4(c) shows the N_2 adsorption isotherms of a pristine CNT buckypaper, 25 wt.% AC coated buckypaper and pure active carbon. The measurement was performed at 77 K in a range of 10^{-6}–1 atm after pre-evacuation for 10 h at 433 K. The hybrid buckypaper exhibits a 3 times higher BET specific area (114.3 $m^2\ g^{-1}$) than the pristine buckypaper (14.1 $m^2\ g^{-1}$), while the specific area of the pure active carbon is 326.4 $m^2\ g^{-1}$. The pore distributions of the three samples are shown in Fig. 4(d). It reveals that the increase of the specific area for the hybrid buckypaper could be attributed to the narrow pore size distribution (average size 4–5 nm) in the AC coating, which also confirmed the role of pore-maker $Zn(Ac)_2$.

The electrochemical performance of buckypaper electrodes was performed in 6 M KOH aqueous solution. Fig. 5(a) shows the cyclic voltammetric (CV) curves of six kinds of buckypaper electrodes with different AC contents at a rapid scan rate of 200 mV s^{-1}. All the CV curves appear quasi-rectangular shape. This indicates a typical characteristic of a double-layer charge/discharge at the electrode interface for our buckypapers. Principally, the specific capacitance is proportional to the area encircled by a CV curve [26]. As shown in Fig. 5(a), the integrated area for the electrodes increased with the increase of AC percentage when it was less than 25 wt.% and then turned to drop when the AC content further increased and lost almost 1/3 of its maximum when the AC content became 100 wt.%. Meanwhile, its CV curve deformed gradually from a rectangle shape to a diamond shape, implying that the excessive AC wrapping may worsen the electrochemical capacitive performance of the hybrid buckypaper electrode at high scanning rate [27]. This is consistent with the conductivity results of the hybrid buckypapers. By contrast, under a low scanning rate such as at 5 mV s^{-1}, the AC coating did not show such a negative effect even in its percentage range from 25 to 100 wt.% (see Fig. S2 in the supplementary material). The corresponding specific capacitance derived from the hybrid buckypaper with 25 wt.% AC at the scan rate of 5 mV s^{-1} was calculated as 110 F g^{-1}, much higher than the pressed CNT/mesoporous carbon powder electrode (60.2 F g^{-1}) at the same scan rate [13]. It revealed that the pre-constructed CNT conductive network tended to be more effective to improve the electrode performance.

Fig. 5(b) illustrates the specific capacitance of the buckypaper electrodes under different charge/discharge current densities. The results agreed well with those from CV curves. The pristine CNT buckypaper shows very low specific capacitance of 10 F g^{-1} at the current density of 0.5 A g^{-1}, which is due to the raw CNTs with large diameter (50–150 nm) induced the low specific area of the buckypapers. When the current density was lower than 2 A g^{-1}, higher AC percentage led to the larger specific area and therefore the higher specific capacitance of the hybrid buckypaper electrodes. However, when the current density was increased above 5 A g^{-1}, the specific capacitance of the hybrid buckypaper decreased with the increase of AC loading amount when larger than 25 wt.%. Thus the buckypaper loading with 25% AC showed the highest electrochemical capacitance at large densities. Moreover, its specific capacitance could be better maintained with the increase of current density, indicative of a better rate performance. Therefore it reveals that the electrode performance of the hybrid buckypaper did not monotonously increase with the AC wrapping

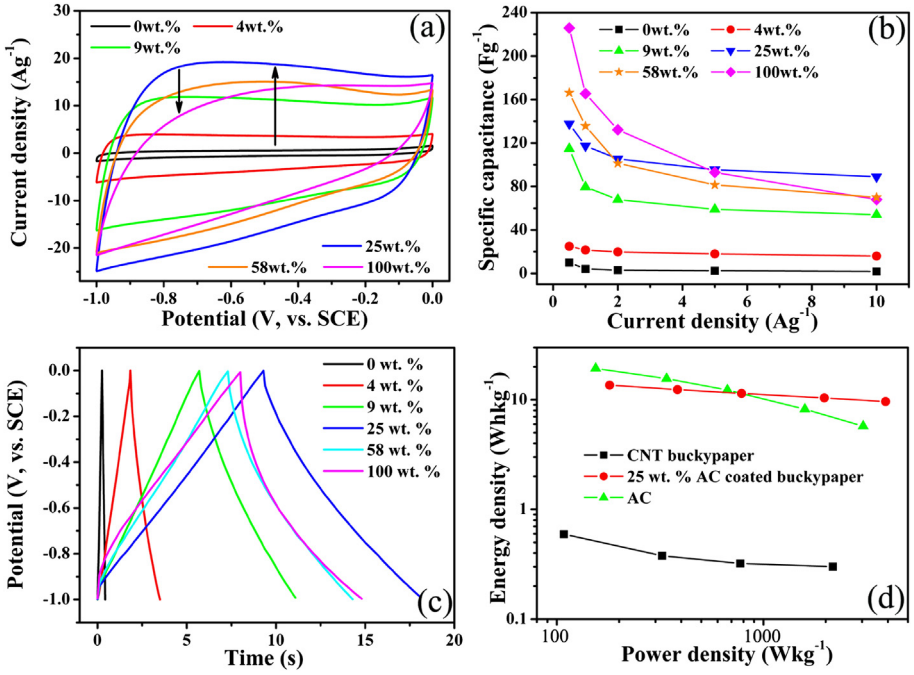

Fig. 5. Cyclic voltammetry curves at a scan rate of 200 mV s^{-1} (a); ratio curves of buckypapers coated with different percent of AC (b); charge/discharge curves of buckypapers coated with different percent of AC at the current density of 10 A g^{-1} (c); Ragone plots of AC, CNT buckypaper and 25 wt.% AC coated buckypaper (d).

percentage, and 25 wt.% is an optimal wrapping amount, in a good agreement with the result from CV curves obtained under different scanning rates shown in Fig. S3. Furthermore, the charge/discharge curves of buckypapers coated with different percent of AC at the current density of 10 A g^{-1} shows that 25 wt.% AC coated buckypaper has a low IR loss value (66.2 mV) and a large columbic efficiency (95.7%) with a well symmetrical curve, as shown in Fig. 5(c). While the IR loss value and the columbic efficiency of pure AC electrode are 137.9 mV and 83%, respectively. That could be attributed to the high electron mobility in the CNT network of the hybrid buckypaper.

The corresponding energy density and power density of the three kinds of electrodes including the pristine CNT buckypaper, pure AC and hybrid buckypaper were calculated according to the charge/discharge curves [10], as shown in Fig. 5(d). The pristine buckypaper presents a quite low energy density due to its low specific surface area and inactive surface. While the pure AC electrode exhibits higher energy density than other two materials in the range of lower power density. However, different from the pure AC electrode, the hybrid buckypaper shows a stable energy density around 10 Whkg^{-1} in a broad range of power density from 200 to 4000 Wkg^{-1}. Thus under the same power density of 4000 Wkg^{-1}, the hybrid buckypaper shows an energy density of 9.6 Whkg^{-1}, nearly six times higher than literature work, in which single-walled CNTs (SWCNTs)/AC electrode (1.6 Whkg^{-1}) was synthesized by the carbonization of the mixture of PAN solution with SWCNT powder [16].

Electrochemical impedance spectroscopy (EIS) analysis is conducted to further understand the mass and charge transfer behaviors at electrode interface [28]. Fig. 6(a) shows the Nyquist plots of the three electrodes (CNT buckypaper, AC and hybrid buckypaper) in 6 M KOH aqueous solution. All of the three Nyquist plots were featured with two distinct parts, a semicircle at high frequencies and a linear line at low frequencies [29]. At high frequencies, the charge transfer resistance (R_{ct}) of the electrode can be obtained from the radius of the semicircle in the Nyquist plot, which is associated with the electron transport at electrode interface [30]. The results show that the R_{ct} hybrid buckypaper lies between the pristine buckypaper and pure AC, agreeing well with their measured electrical conductivity sequence. The smaller R_{ct} for the hybrid buckypaper than it for the pristine AC should be attributed to the CNT conductive network and the good interfacial contact between AC and CNT, which can enhance the electron transferring between the two materials. In the Nyquist plot, the transition region between the semicircle at high frequencies and a linear line at low frequencies, which is relative to the electrolyte diffusion resistance (EDR) in Warburg impedance, shows the property of the porous structure in EDLC [31]. Lower EDR means better porous structure for the wettability toward electrolyte. As shown in Fig. 6(a), the hybrid buckypaper evidently exhibits a lower EDR than pristine AC. Furthermore, the Bode plots of the three samples (shown in Fig. S5) indicate that the hybrid buckypaper has a higher phase angle at low frequencies, which is close to 90°, suggesting a favorable electrochemical double layer in the interface between the electrode and the electrolyte [32]. As a result, this hybrid buckypaper shows a stable cyclic performance at a large current density of 5 A g^{-1}, as is shown in Fig. 6(b). Its specific capacitance keeps 98% of the initial value after 4000 cycles.

The significant increase of specific capacitance is attributed to the effective combination of AC's high electrochemical activity and CNT's high electric conductivity [33]. It's more likely that the separated electrons formed on the AC thin layer can transfer fast to CNT network. Furthermore, the CNT network possesses abundant interconnected porous structures, which are helpful for electrolyte pass-through and ionic diffusion. Although pure AC has low electron mobility, it's still able to transfer sufficient electrons to the electrode interface at low current densities. When the current density is greatly increased, the large surface area of the AC electrode ensures massive ionic charges in the electrolyte to rapidly accumulate to the surface of the electrodes, but the electrons will be kind of difficult to respond and transport promptly to form the electrochemical double layer due to the low conductivity of AC, and therefore suppressing its power density. The AC coated CNT buckypaper structure tends to be a promising architecture to overcome these drawbacks, and achieve the compromise of high power density and high energy density. The CNTs plays a role as the micro current collector in the hybrid electrode. The better interface between the AC and the CNT facilitates electrons to go through more effectively than the simple mixing of the two materials. It's also proved that the mixture electrode composed of 75 wt.% CNTs and 25 wt.% AC shows a worse electrochemical performance than the 25 wt.% AC coated CNT buckypaper hybrid electrode as is shown in Fig. S6. The integrated area for the mixture electrode displays less than 1/2 of the area for the hybrid electrode at the scan rate of 200 mV s^{-1} (see Fig. S6(a)). And its specific capacitance is only 1/3 of the hybrid electrode at the current density of 10 A g^{-1} (see Fig. S6(B)). It could be inferred that the coating of thin layer of low conductive AC on buckypaper formed a compact interface between AC and CNT. Hence the charges accumulated on AC/electrolyte interfaces can smoothly transfer through the AC layer and the interface to conductive CNT network and be wired out to collectors. As a result, with a suitable thickness of AC coating, conductive CNT network helps exploit the electrochemical capacitive performance of AC layer to a large extent.

The CV curves of the assembled EDLC using the hybrid electrodes with a total mass of the opposite electrodes as 10 mg are shown in Fig. 7(a). The curve could keep as a rectangle at the scan

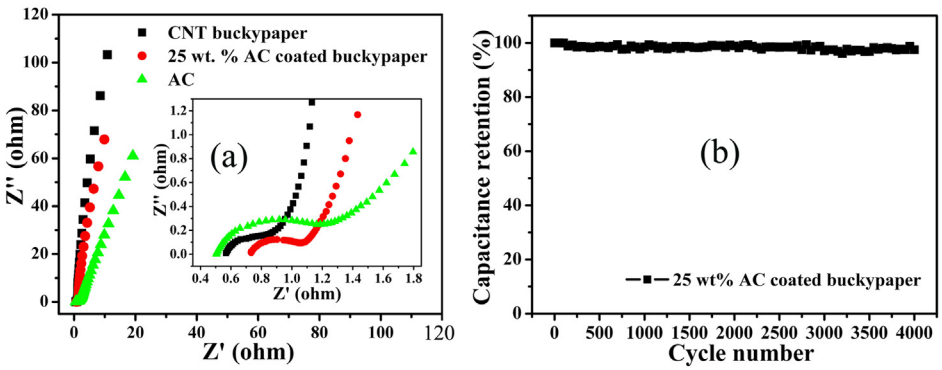

Fig. 6. Nyquist plots (the insert shows an enlarged view) of CNT buckypaper, AC and 25 wt.% AC coated buckypaper (a); cycling performance of 25 wt.% AC coated buckypaper at a current density of 5 A g^{-1} (b).

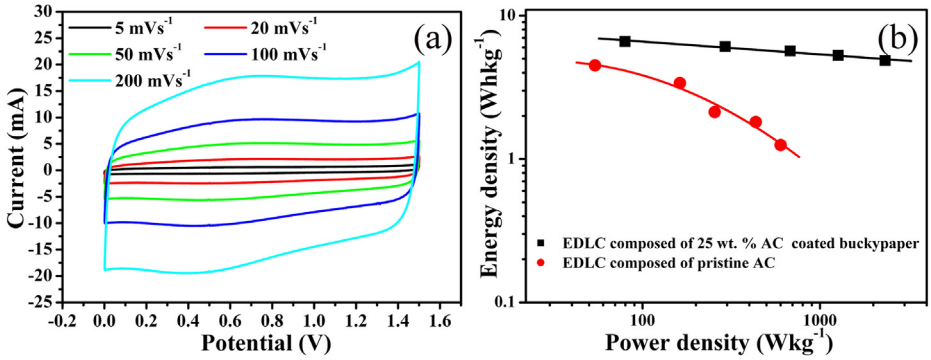

Fig. 7. Cyclic voltammetry curves (a) and Ragone plot (b) of an electrochemical capacitor fabricated with 25 wt.% AC coated buckypaper electrodes.

rate from 5 to 200 mV s^{-1}. That should be attributed to the better charge exchange between AC and CNTs, and high conductivity inner the electrodes. As a result, the energy density of the hybrid buckypaper supercapacitor shows a slight drop along with the increase of power density, while it of the pristine AC supercapacitor largely decreases, as shown in Fig. 7(b).

4. Summary

A thin layer of AC has been uniformly wrapped on the conductive CNT network by a easy infiltration route, where buckypapers were soaked with PAN-$Zn(Ac)_2$/DMF solution and then carbonized. The porous AC wrapping can prominently improve the electrochemical capacitive performances of the buckypaper, especially under high current densities. Such performance enhancement is attributed to the effective combination of the high capacitance of AC coating and the fast electron transport along robust CNT network in the hybrid buckypaper. The hybrid structure is liable to be scaled up and may serve as a promising approach for low cost and high-performance energy storage devices with easily manipulated paper electrodes.

Acknowledgments

The project was supported by the National Basic Research program (2010CB934700), the Key Program of the National Science Foundation of China (No.10834004), the Science and Technology Project of Suzhou, China (SYG201018) and Production and Research Collaborative Innovation Project of Jiangsu Province, China (BY2011178).

Appendix A. Supplementary data

Supplementary data related to this article can be found at http://dx.doi.org/10.1016/j.jpowsour.2013.02.082.

References

[1] P. Simon, Y. Gogotsi, Nat. Mater. 7 (2008) 845–854.
[2] J. Gamby, P.L. Taberna, P. Simon, J.F. Fauvarque, M. Chesneau, J. Power Sourc. 101 (2001) 109–116.
[3] P. Sharma, T.S. Bhatti 51 (2010) 2901–2912.
[4] D. Tashima, E. Yamamoto, N. Kai, D. Fujikawa, G. Sakai, M. Otsubo, et al., Carbon 49 (2011) 4848–4857.
[5] P. Barpanda, G. Fanchini, G.G. Amatucci, Carbon 49 (2011) 2538–2548.
[6] S.L. Candelaria, Y. Shao, W. Zhou, X. Li, J. Xiao, J. Zhang, et al., Nano Energy 1 (2012) 195–220.
[7] C.X. Guo, X.M. Li, Energy Environ. Sci. 4 (2011) 4504–4507.
[8] J. Yan, T. Wei, B. Shao, F. Ma, Z. Fan, M. Zhang, et al., Carbon 48 (2010) 1731–1737.
[9] Z. Lei, N. Christov, X.S. Zhao, Energy Environ. Sci. 4 (2011) 1866–1873.
[10] G. Xu, C. Zheng, Q. Zhang, J. Huang, M. Zhao, J. Nie, et al., Nano Res. 4 (2011) 870–881.
[11] W. Lu, R. Hartman, L. Qu, L. Dai, J. Phys. Chem. Lett. 2 (2011) 655–660.
[12] B. Yi, X. Chen, K. Guo, L. Xu, C. Chen, H. Yan, et al., Mater. Res. Bull. 46 (2011) 2168–2172.
[13] X. Qian, Y. Lv, W. Li, Y. Xia, D. Zhao, J. Mater. Chem. 21 (2011) 13025–13031.
[14] M.C. Gutierrez, D. Carriazo, A. Tamayo, R. Jimenez, F. Pico, J.M. Rojo, et al., Chem. Eur. J. 17 (2011) 10533–10537.
[15] F. Béguin, K. Szostak, G. Lota, E. Frackowiak, Adv. Mater. 17 (2005) 2380–2384.
[16] T. Liu, T.V. Sreekumar, S. Kumar, R.H. Hauge, R.E. Smalley, Carbon 41 (2003) 2440–2442.
[17] M. Noked, S. Okashy, T. Zimrin, D. Aurbach, Angew. Chem. Int. Ed. 51 (2012) 1568–1571.
[18] S.C. Hawkins, J.M. Poole, C.P. Huynh, J. Phys. Chem. C 113 (2009) 12976–12982.
[19] M. Endo, H. Muramatsu, T. Hayashi, K.A. Kim, M. Terrones, M.S. Dresselhaus, Nature 433 (2005) 476.
[20] Q. Guo, X. Zhou, X. Li, S. Chen, A. Seema, A. Greiner, et al., J. Mater. Chem. 19 (2009) 2810–2816.
[21] C. Kim, B.T.N. Ngoc, K.S. Yang, M. Kojima, Y.M. Kim, Y.J. Kim, et al., Adv. Mater. 19 (2007) 2341–2346.
[22] A. Izadi-Najafabadi, T. Yamada, D.N. Futaba, M. Yudasaka, H. Takagi, H. Hatori, et al., ACS Nano 5 (2011) 811–819.
[23] I. Ivanov, A. Puretzky, G. Eres, H. Wang, Z. Pan, H. Cui, et al., Appl. Phys. Lett. 89 (2006) 223110.
[24] R. Saito, A. Gruneis, G.G. Samsonidze, V.W. Brar, G. Dresselhaus, M.S. Dresselhaus, et al., New J. Phys. 5 (2003) 157.1–157.15.
[25] Z. Xie, R.J. White, J. Weber, A. Taubert, M.M. Titirici, J. Mater. Chem. 21 (2011) 7434–7442.
[26] J.W. Lee, T. Ahn, D. Soundararajan, J.M. Ko, J. Kim, Chem. Commun. 47 (2011) 6305–6307.
[27] K. Xie, X. Qin, X. Wang, Y. Wang, H. Tao, Q. Wu, et al., Adv. Mater. 24 (2012) 347–352.
[28] J.R. Miller, R.A. Outlaw, B.C. Holloway, Science 329 (2010) 1637–1639.
[29] S.H. Aboutalebi, A.T. Chidembo, M. Salari, K. Konstantinov, D. Wexler, H.K. Liu, et al., Energy Environ. Sci. 4 (2011) 1855–1865.
[30] Y. Lin, T. Wei, H. Chien, S. Lu, Adv. Energy Mater. 1 (2011) 901–907.
[31] Z. Weng, Y. Su, D. Wang, F. Li, J. Du, H. Cheng, Adv. Energy Mater. 1 (2011) 917–922.
[32] T. Hiraoka, A. Najafabadi, T. Yamada, D.N. Futaba, S. Yasuda, O. Tanaike, et al., Adv. Funct. Mater. 20 (2010) 422–428.
[33] M.N. Hyder, S.W. Lee, F.C. Cebeci, D.J. Schmidt, Y. Shao-Horn, P.T. Hammond, ACS Nano 5 (2011) 8552–8561.